AGU PUBLICATIONS

Earth's Future

RESEARCH ARTICLE

10.1002/2015EF000331

Special Section:
Integrated field analysis & modeling of the coastal dynamics of sea level rise in the northern Gulf of Mexico

Key Points:
- Long-term shoreline change and dune height are jointly correlated to sea-level rise
- A dune-height constraint improves the shoreline-change prediction confidence
- Forecasts increase shoreline-change uncertainty and reduce dune-height uncertainty

Corresponding author:
N. G. Plant, nplant@usgs.gov

Citation:
Plant, N. G., E. Robert Thieler, and D. L. Passeri (2016), Coupling centennial-scale shoreline change to sea-level rise and coastal morphology in the Gulf of Mexico using a Bayesian network, *Earth's Future*, *4*, 143–158, doi:10.1002/2015EF000331.

Received 18 OCT 2015
Accepted 30 MAR 2016
Accepted article online 4 APR 2016
Published online 2 MAY 2016

Coupling centennial-scale shoreline change to sea-level rise and coastal morphology in the Gulf of Mexico using a Bayesian network

Nathaniel G. Plant[1], E. Robert Thieler[2], and Davina L. Passeri[1]

[1]U.S. Geological Survey, Saint Petersburg, Florida, USA, [2]U.S. Geological Survey, Woods Hole, Massachusetts, USA

Abstract Predictions of coastal evolution driven by episodic and persistent processes associated with storms and relative sea-level rise (SLR) are required to test our understanding, evaluate our predictive capability, and to provide guidance for coastal management decisions. Previous work demonstrated that the spatial variability of long-term shoreline change can be predicted using observed SLR rates, tide range, wave height, coastal slope, and a characterization of the geomorphic setting. The shoreline is not sufficient to indicate which processes are important in causing shoreline change, such as overwash that depends on coastal dune elevations. Predicting dune height is intrinsically important to assess future storm vulnerability. Here, we enhance shoreline-change predictions by including dune height as a variable in a statistical modeling approach. Dune height can also be used as an input variable, but it does not improve the shoreline-change prediction skill. Dune-height input does help to reduce prediction uncertainty. That is, by including dune height, the prediction is more precise but not more accurate. Comparing hindcast evaluations, better predictive skill was found when predicting dune height (0.8) compared with shoreline change (0.6). The skill depends on the level of detail of the model and we identify an optimized model that has high skill and minimal overfitting. The predictive model can be implemented with a range of forecast scenarios, and we illustrate the impacts of a higher future sea-level. This scenario shows that the shoreline change becomes increasingly erosional and more uncertain. Predicted dune heights are lower and the dune height uncertainty decreases.

1. Introduction

Decadal to centennial scale coastal change integrates many processes, some of which take place over long time periods, such as relative sea-level rise (SLR, which includes eustatic, isostatic, and other climatic and non-climatic effects [*Church et al.*, 2013]), and some of which take place over very short time periods, such as during storms. Long-term shoreline change along low-lying coastal barrier islands like those found along the U.S. Gulf of Mexico can be extremely rapid, with erosion rates exceeding 10 m/year (Figure 1). These extreme rates of erosion almost certainly involve both high rates of relative SLR [*Penland et al.*, 1988; *Morton et al.*, 2004] and storms [*Fearnley et al.*, 2009; *Stockdon et al.*, 2012]. Long-term shoreline change also depends on the local sediment budget and sediment texture, such that barrier islands with less available sediment and finer sediments will erode more quickly than barriers with abundant or coarse sediment [*Twichell et al.*, 2009; *Twichell et al.*, 2013].

Short-term storm impacts that affect shoreline change are largely controlled by the height of dunes [*Sallenger*, 2000; *Stockdon et al.*, 2007; *Long et al.*, 2014], which controls the frequency of overwash, dune erosion, and landward barrier migration or rollover. The details of exactly how much shoreline change might result from a particular storm depend on a number of other factors such as beach width, dune width, and island width [*Donnelly et al.*, 2006; *Plant and Stockdon*, 2012]. These details can be accounted for with detailed numerical models [*Roelvink et al.*, 2009; *Lindemer et al.*, 2010; *Mccall et al.*, 2010; *Sherwood et al.*, 2014] if the topography, bathymetry, and storm conditions are known, which tends to be true only after storms have occurred but not for future conditions. For future projections, storm processes and SLR can be coupled in a number of ways to predict barrier island evolution [*Stolper et al.*, 2005; *Lorenzo-Trueba and Ashton*, 2014]. These models all require extracting a number of calibration parameters from observations. The parameters often have relatively high uncertainties [*Apotsos et al.*, 2008] and the calibration data

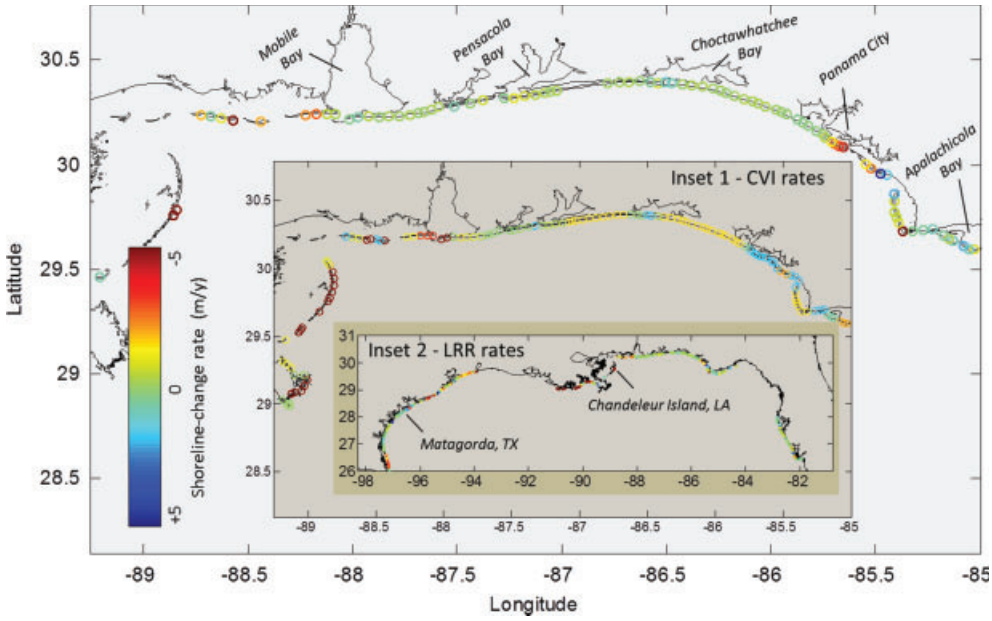

Figure 1. Shoreline-change rates based on a linear regression (linear regression rate [LRR]) analysis that included shorelines observed through 2002 [*Miller et al.*, 2004] (main figure) and change rates based on a synthesis (coastal vulnerability index [CVI]) of studies [*Gutierrez et al.*, 2014] (inset 1). Both data sets span the U.S. Gulf of Mexico coastline (inset 2).

themselves (e.g., measured shoreline changes) also have substantial uncertainties [*Moore et al.*, 2006; *Passeri et al.*, 2014].

Other influences on shoreline change in this region result from societal processes, such as artificial berm-building [*Plant et al.*, 2014] and ecosystem restoration in response to recent hurricanes and impacts of the Deepwater Horizon oil spill [*Gulf Coast Ecosystem Restoration Council*, 2014]. The restoration efforts are intended to increase the economic and ecologic sustainability of the Gulf of Mexico coast, and they typically consider storms, SLR, and associated land loss. The threats posed by SLR to sustainability have been investigated in a number of ways, often related to flooding of the current coastal landform [*Smith et al.*, 2010; *Mousavi et al.*, 2011; *Hagen and Bacopoulos*, 2012; *Atkinson et al.*, 2013]. We wish to predict how aspects of that landform will change as sea level changes. For example, changing sea-level and landforms affect tides and hurricane storm surge dynamics [*Bilskie et al.*, 2014; *Passeri et al.*, 2015a, 2015b]. These hydrodynamic analyses require a definition of the shoreline as lateral boundaries in the model domains and elevations are required along barrier islands to account for how these boundaries might be inundated. We develop and test a model that simultaneously predicts shoreline-change rates and dune height by coupling historical observations of these variables to SLR, wave height, and tides, and geomorphic classification data sets.

A previous approach used a statistical model to test the coupling of these variables and showed that SLR and geomorphology were most important for predicting the variability of shoreline change [*Gutierrez et al.*, 2011]. This model was applied across all U.S. Coastlines [*Gutierrez et al.*, 2014] where hindcast predictions were shown to have about a 70% success rate. But, when just the Gulf Coast was considered, the success rate was only about 30%. For the previous model, the geomorphology was classified in five broad categories, only one of which included barrier islands. Because much of the Gulf of Mexico is described by this one category, different geomorphologies along the Gulf of Mexico coast were not distinguished and potentially important relationships between geomorphology and the other variables were not resolved. We augment the geomorphic description with historical averages of the dune-crest height to make simultaneous predictions of shoreline change and dune height. We investigate the potential to improve shoreline-change predictions. We will show that there is substantial spatial variability in these variables, and that we must estimate this variability as well as the joint correlations between shorelines, dunes, and SLR. We then test predictions of historical shoreline-change rates and dune heights driven by spatial variability in relative SLR

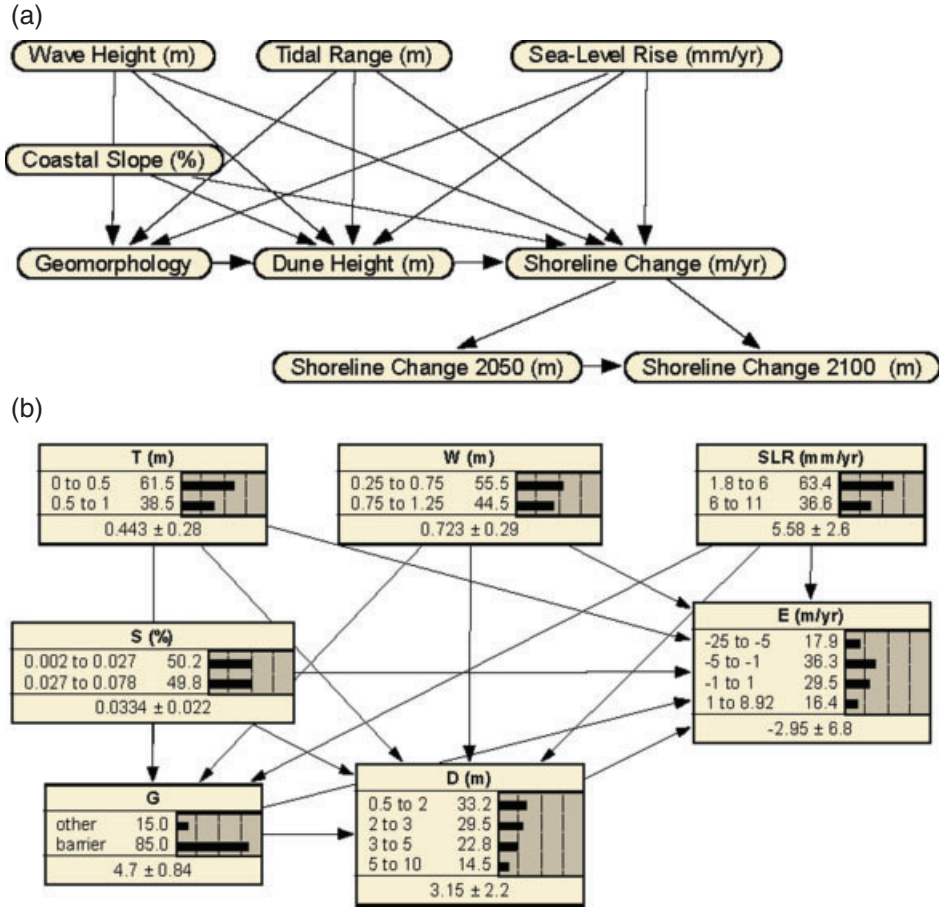

Figure 2. (a) Conceptual model for predicting dune height, shoreline change rates, and shoreline changes in the years 2050 and 2100 driven by sea-level rise (SLR), tide range, wave height, coastal plain slope, and geomorphologic classification and (b) the discretized model implementation. (The shoreline changes at 2050 and 2100 are included in the model, but are not shown in (b).)

and develop a method for extending the hindcast predictions to forecast scenarios that show how dune height affects shoreline change (and vice versa) under two alternative SLR scenarios.

2. Methods

2.1. Statistical Model

Based on several previous modeling approaches [*Gutierrez et al.*, 2011, 2014], we use a Bayesian network (BN) to develop a predictive model for future dune-height, shoreline-change rate, and shoreline positions that are driven by SLR and conditioned on two other oceanographic variables (tide range and wave height, averaged over historical records) and the coastal-plain slope and geomorphic classification (which, as mentioned earlier is not particularly informative in this study area because the majority of the cases fall in a single class: barrier islands). The model (Figure 2) accounts for joint correlations between some of the variables (shown graphically in Figure 2b) such that

$$P\left(E_i\right) = \sum_{\beta,G,D,\mathrm{SLR},T,W} P\left(E_i, \beta, G, D, \mathrm{SLR}, T, W\right) \tag{1a}$$

where the left side of equation (2a) represents the marginal distribution, which is the probability of a particular shoreline-change rate, $P(E_i)$, given the joint probability distribution with the other variables (β = broad-scale coastal slope, G = geomorphic classification, D = dune height, SLR, T = tide range, and W = wave height). The dune-height variable is based on an average of values extracted from lidar surveys over the past decade [*Stockdon et al.*, 2012] and the other variables are described by *Thieler and Hammar-Klose* [1999]. The index, i, denotes a discrete range of shoreline-change rates (Figure 2b), and the full range of observed values are divided into this set of discrete ranges, or bins. The summation is over all

input variables, which are also divided into discrete bins. The BN stores the joint probability information in tables that describe the conditional probability of each variable given the state value (bin) of the other variables (Figure 2). Thus, the conditional relationships are decomposed as follows:

$$P\left(E_i\right) = \sum_{\beta,G,D,\mathrm{SLR},T,W} P\left(E_i|D,G,\beta,\mathrm{SLR},T,W\right) P\left(D|G,\beta,\mathrm{SLR},T,W\right) P\left(G,|\beta,\mathrm{SLR},T,W\right) P\left(\beta\right) P\left(\mathrm{SLR}\right) P\left(T\right) P\left(W\right) \tag{1b}$$

where the last four terms (probabilities of β, SLR, T, and W) are external inputs that are treated as if they were statistically independent of each other. Shoreline-change rate, dune height, and geomorphology depend on each other and on the external inputs. In our case, geomorphology for the Gulf of Mexico distinguished barrier islands from mainland coastlines and more detail about the geomorphology is added by including the dune-height variable. In this form, a prediction of the probability of shoreline change occurring in each of several ranges ($i = 1, 2, 3, 4$; see Figure 2b) can be computed. Equation 1b can be re-arranged to get a similar prediction for dune height, using Bayes rule:

$$P\left(D_i\right) = \sum_{E} P\left(E,|D_i,G,\beta,\mathrm{SLR},T,W\right) P\left(D_i\right) / P\left(E\right) \tag{2}$$

where the index, i, indicates the discrete ranges of dune heights ($i = 1, 2, 3, 4$; see Figure 2b) and the summation is over all shoreline-change rates after using 1b. These equations allow prediction of shoreline change by specifying the probability of all the other variables including or omitting dune height as an input. Dune height can be predicted, either including or excluding shoreline-change probabilities. If no conditional constraints are supplied, shoreline-change rate and dune height (and all the other variables) are predicted with prior distributions, which simply represent the frequency of occurrence of each variable's value in the data set that is used to estimate the conditional probabilities. Finally, the prediction of the change in shoreline position, $\Delta = \tau E$, at any point in time is

$$P\left(\Delta_j\right) = \sum_{i} P\left(E_i\right)_{\tau\ E_i=\Delta_j} \tag{3}$$

where τ is the elapsed time since some reference time. We use 2010 as the reference time. Equation 3 redistributes probability defined for each E_i onto discrete values of Δ_j, where the index j refers to the members of the discrete set of Δ values that are included in the model. For 2050 (Figure 2a), this set included the values [−1000, −100, −50, 50, 100, 500] m. For 2100, this set was expanded to include [−2500, −750, −500, −250, −100, −50, 50, 100, 250, 500, 1000] m.

2.2. Data

The conditional probabilities required by the BN can be estimated from data sets and model calculations. Two data sets contain estimates of historical shoreline change along the Gulf of Mexico coast (Figure 1) and we include both in order to identify uncertainties in shoreline-change information and to test for differences in predictability resulting from using one or the other as inputs (e.g., predicting dune height) or to verify model-prediction output. Because the BN requires discretization of each variable into bins (or classes — such as is already the case for geomorphology), we start with a very simple discretization (Figure 2b). In the simple scheme, the inputs (SLR, T, W, β, and G) are given two states (high and low) and the outputs (D and E) are allowed four states. The choice of the number of bins per variable affects the ability of the model to fit the data. Too few bins impede accurate representation of the data and the corresponding joint probability relationships. However, because the model is trained on data, too many bins may lead to model overfitting [*Fienen and Plant*, 2015]. The boundary between bins was chosen somewhat subjectively correspond to apparent threshold values (see Section 3). The sensitivity of the choice of number of bins and bin boundaries is addressed in Section 4.

Shoreline-change data come from an assessment of shorelines at nominally four time periods spanning the mid-1800s to 2002 [*Miller et al.*, 2004; *Morton et al.*, 2004]. The shorelines were used to estimate a long-term change rate using linear regression, hereinafter referred to as the linear regression rate (LRR), at a number of discrete locations (Figure 1). The second data set comes from the same source as was used to develop a BN model for the entire U.S. coastline [*Gutierrez et al.*, 2014], which included shoreline-change rates nominally spanning the past 100 years and incorporated data used to develop a coastal vulnerability index (CVI) [*Thieler and Hammar-Klose*, 1999]. We discretized the shoreline changes into four bins (Figure 2b) to resolve

extreme erosion (<−5 m/year), moderate erosion (−5 to −1 m/year), no change (−1 to 1 m/year), and accretion (>1 m/year). The *Gutierrez et al.* [2014] data set also included estimates of relative SLR, tide range, wave height, slope, and geomorphology, which we used with both of the shoreline-change rate data sets by spatial interpolation to nearby points in the LRR data set. The BN is tolerant of missing data and hence, we did not attempt to interpolate where the nearest data were missing. The BN learns conditional probabilities through fitting the data that are not missing. Predictions from the BN replace missing data with the prior distributions, which generally leads to increased uncertainty in predictions at locations where data are missing.

Comparing the data across the entire Gulf of Mexico region (Figure 1, inset 2) shows that there are some differences between the two shoreline-change data sets (Figure 3), with a correlation between the two explaining only 39% of the variance of the LRR. Nonetheless, when the synthesis rates (hereinafter called CVI rates) are less than −5 m/year, the LRR rates are likely to represent extreme erosion. And both data sets show correspondence for no-change and accretion. It is not clear which data set is most useful for capturing the joint correlations between shoreline change and the other variables, hence, we will retain both and explain differences in the uncertainty with the BN. The broad correlation of the shoreline-change rates with SLR is very similar between the two data sets (Figure 3b), and this suggests that the differences between the two data sets may not affect the predictions. For low SLR, the shoreline-change rates are generally low and are more negative (e.g., erosion), but are more variable for higher SLR.

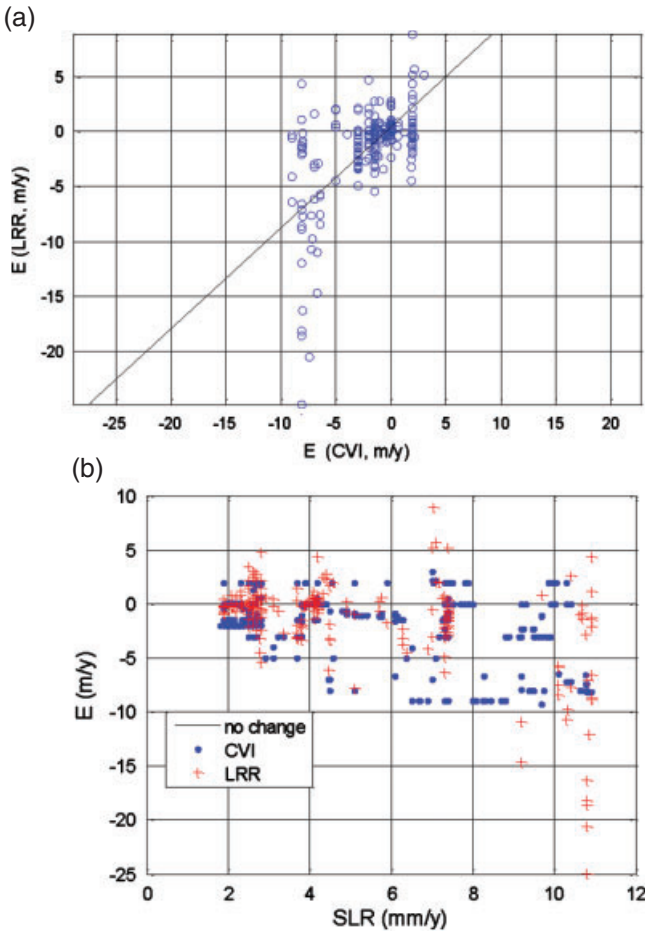

Figure 3. Comparison of (a) shoreline change rate, *E*, estimates from the long-term regression (LRR) and the coastal vulnerability index (CVI) and (b) comparison of shoreline-change rates to sea-level rise (SLR). The solid line in (a) indicates perfect agreement.

The dune-height data were obtained from an analysis of the Gulf Coast's storm vulnerability [*Stockdon et al.*, 2012]. The dune-height is the height of the primary dune crest relative to mean sea level and we averaged data where there were multiple estimates, which come from baseline studies and re-surveys associated with specific storms [*Doran et al.*, 2009; *Sallenger et al.*, 2009; *Mccall et al.*, 2010; *Plant et al.*, 2010; *Guy et al.*, 2013]. Dune-height data were extracted from airborne lidar acquired during the time period between 2002 and 2012. Thus, the dune-height data are averaged over a much shorter time period than the shoreline-change data, but we found that the dune heights depended on the longer-term parameters (Figure 4), implying that there is a systematic relationship that can be exploited for prediction and that current dune heights are relevant to the future response of the coast. In particular, where dune height exceeded 3–4 m, the long-term shoreline-change rates were generally small. Where dune height was low, shoreline-change rates could be extremely erosional (<−5 m/year) but could also be accretional (>1). For SLR exceeding 5 mm/year, dunes tend to be low (Figure 4b). We will test for systematic relationships that we could capture in the statistical model.

2.3. Model Testing

The BN is trained on the data sets described in the previous section to make estimates of the terms required in equations (1a)–(3). We use the expectation maximization method within the Netica software package [*Norsys Software Corp*, 2012] to train the model. This method iteratively updates the conditional probabilities by first estimating the expected value of the likelihood function given the current conditional probabilities and then maximizing this expected value by varying the conditional probabilities until the expected likelihood converges [*Dempster et al.*, 1977; *Lauritzen*, 1995]. Once trained, the model can be tested against data to see how well the joint correlations can explain the spatial variability of the data. We perform four tests, each having several variations to explore sensitivity to parameters. The first test is a hindcast prediction of the shoreline-change rates given all of the other variables, compared to the LRR and the CVI shoreline-change rates, and either including or excluding the dune height as a constraint. The second test is a hindcast prediction of the dune height, using either the LRR or CVI rate as input, or omitting the shoreline-change input. The third test explores the robustness of the BN to an increase in complexity by increasing the number of discrete ranges for the input from two bins to six bins. We use a calibration/validation approach that withholds data from the training and tests on both the training and withheld validation data [*Fienen and Plant*, 2015]. We withheld one-third of the data, trained on the remaining two-thirds, and repeated (bootstrapped) for all permutations of training and withheld sets. Finally, we conduct a sensitivity test for predictions of future shoreline position and dune height (and corresponding uncertainty) by applying different SLR scenarios rather than using the historical values.

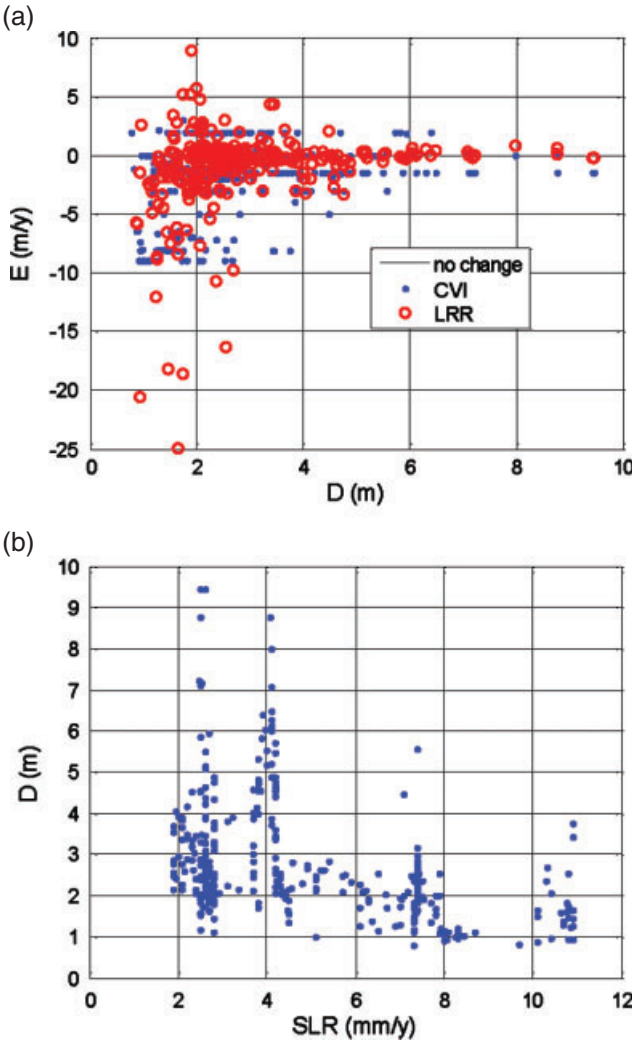

Figure 4. Comparison of dune height, *D*, to (a) shoreline-change rate, *E*, and to (b) sea-level rise (SLR).

The predictions are not the values of each parameter, but are instead the probability that the value falls within each bin. To compare to observed values, we must convert the prediction to a Bayesian-mean (i.e., $\bar{E} = \sum E_i p[E_i]$) and standard deviation (σ). The standard deviation can be used as a weight such that predictions that are uncertain (high standard deviation) are weighted less than confident predictions. We report the skill of the correlation between the mean of the prediction using the weights and without the weights. The skill is computed as

$$\text{Skill} = 1 - \frac{\text{msr}}{\text{msd}} \tag{4}$$

where msr is the mean-square residuals of the linear regression between the Bayesian-mean value and the data, and msd is the mean-square of the data. The weights are applied to each data value in calculating the mean-square values: $\text{msd} = d^T Q\, d$ [*Priestly*, 1981], where d is the data vector, Q is a diagonal matrix with

elements $(n\,\sigma^2)^{-1}$, and n is a normalizing coefficient so that the sum of the weights equals unity. Predictions with large uncertainties are weighted less than more confident predictions in this calculation. If both the Bayesian-mean values and the Bayesian uncertainty are accurate, the weighted skill will be higher than the unweighted skill. The maximum skill is unity. The unweighted skill is computed by replacing σ with unity. Another way to measure the skill of the prediction is to compare it to the prior probabilities to assess whether constraining the prediction with inputs actually increases the certainty. We use the likelihood ratio (LR) [*Weigend and Bhansali*, 1994] to measure the change in certainty:

$$\mathrm{LR} = \sum log\,\{p\,[E\,(k)\,|\mathrm{input}]\} - \sum \log\,\{p\,[E\,(k)]\} \tag{5}$$

where the first term is the updated probability evaluated at the kth observation location and the second term is the probability of the prior at that location. We sum over all locations. Positive LR values indicate improvement over the prior with both accurate predictions and high confidence. Negative LR values indicate either inaccurate but overly confident predictions (i.e., precise but wrong), or excessively uncertain predictions.

3. Results

3.1. Example Scenarios

A trained BN will make a prediction in the form indicated by equations (1a)–(3). Without imposing any conditional probabilities on the input variables, this prediction is called the prior (shown in Figure 2b), which gives probabilities for each variable falling in each bin. Thus, the most likely shoreline-change rate is −5 to −1 m/year (36% likely) and the most likely dune height is 0.5–2 m (33% likely). The prior probabilities for all the variables can be determined from Figure 2b. By constraining some of the variables, the prior probabilities are updated to reflect specific scenarios or conditions at specific locations. For example, Figure 5a shows that if we select a high SLR, low wave height, tide range, and slope and restrict consideration to barrier island geomorphology, the updated prediction is virtually certain that the dunes will be low (0.5–2 m with 99% likelihood) and the most likely shoreline-change rate will correspond to extreme erosion (−25 to −5 m/year with 46% likelihood). However, there is some uncertainty in the shoreline-change prediction and there is significant likelihood of accretion (1–9 m/year with 21% likelihood). Alternatively, we can examine the lower SLR scenario (1.8–6 mm/year) and change the coastal slope to be steeper (also with 100% likelihood). In this scenario, we find that the shoreline-change rate is much more likely to be stable (−1 to 1 m/year with 49% likelihood) and dunes are likely to be higher (>2 m with 91% probability). These examples also illustrate how shoreline change and dune height are predicted simultaneously as we did not constrain either of these variables.

3.2. Hindcasting Evaluation

We can extract inputs from the data set and, at each location, sequentially apply the input as constraints to the BN to extract probabilities of shoreline change and dune height (Figures 6 and 7). Locations are presented from west to east around the U.S. Gulf Coast (Figure 1, inset 2). The first prediction uses all the inputs, including the dune height, and compares to the LRR and CVI shoreline-change data (Figures 6a and 6b, respectively). These results were obtained using the baseline BN (Figure 2b). This shows that predictions can be made everywhere, even if one of the input variables is not constrained (e.g., dune height). Unconstrained data result in the prior being used in the updated prediction. There are variations in the most-likely predictions (indicated by the dark band of the inner 50% of the probability distribution). The BN gives an identical prediction in the comparison to both the LRR and CVI cases because the inputs did not differ. If dune height is removed from the input, the prediction is not changed substantially (Figure 6c), other than reducing the spatial variability in the uncertainty, with more occurrences of relatively high uncertainty. The uncertainty increased markedly in some cases when we remove the additional constraint that is supplied by the dune height (e.g., at the location near longitude 86°, between Choctawhatchee Bay and Panama City, where dunes are relatively high). Thus, shoreline change does not depend uniformly on dune height. Dune height can be predicted in the same manner as shoreline-change rates (Figure 7) where we use either the LRR or CVI shoreline-change rates as input (Figures 7a and 7b, respectively). There are very few differences in the predictions shown in Figures 7a and 7b. The very high dunes found between Choctawhatchee Bay and Panama City are statistically anomalous, exceeding the 95% percentile confidence band. To the west

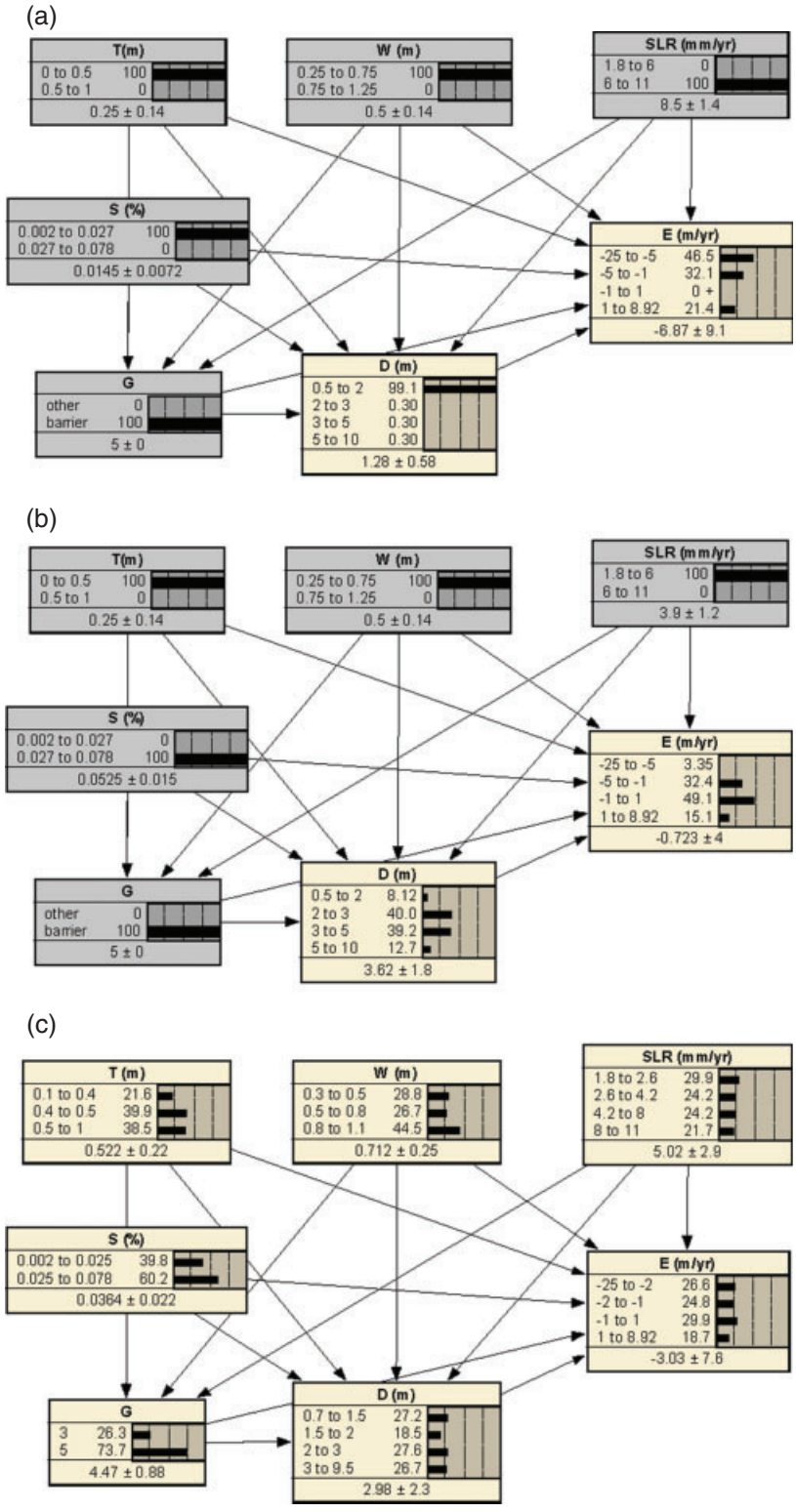

Figure 5. Examples of probabilities predicted by the Bayesian network trained on both linear regression rate and coastal vulnerability index shoreline-change rate data. Constraints are indicated by variables (boxes) that are gray and specify 100% probability in a specific bin. Examples include (a) conditions associated with extreme erosion rates and low dunes, and (b) conditions associated with low erosion rates and high dunes. (c) The optimized model, showing prior predictions.

(longitude 97, near Corpus Christi, TX) there are high dunes that are predicted to be higher than 3 m and the data and predictions are in agreement. If shoreline-change rates are omitted (Figure 7c), there are increases in uncertainties and, as before, less spatial variability in the predictions.

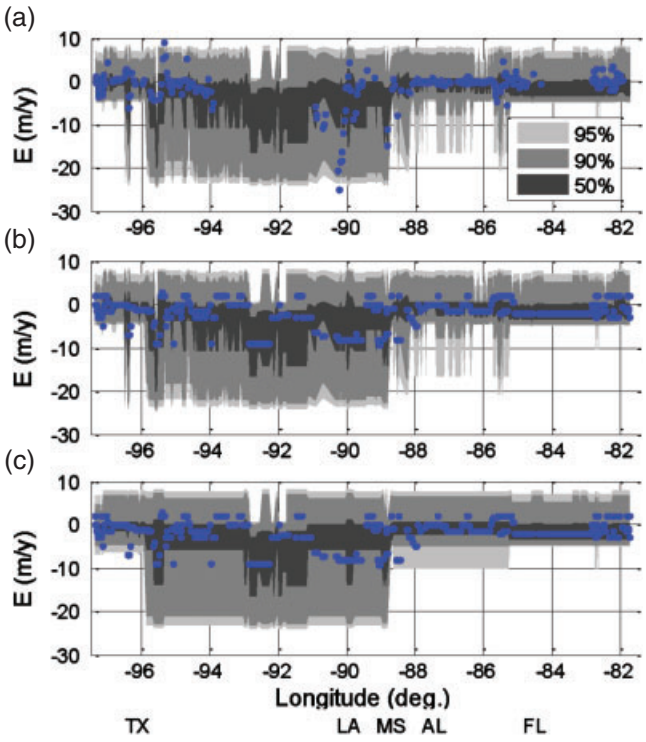

Figure 6. Shoreline-change rate prediction using Bayesian network trained with linear regression rate (LRR) and coastal vulnerability index (CVI) data compared to (a) the LRR data, (b) the CVI data with the dune height as input, and (c) the CVI data predicted without dune-height input. (Note: predictions for (a) and (b) have the same input and are identical.) Shading indicates the 50%, 90%, and 95% confidence intervals of the prediction. Blue dots represent the data. Abbreviations for each coastal state (TX, LA, MS, AL, and FL) are labeled for location reference (and see Figure 1.)

The robustness of the BN predictions was examined by training on LRR or CVI rate data and then testing against these data (Table 1). If the BN is trained on the LRR data it predicts LRR with a weighted skill of 0.6, but predicts the CVI data with a skill of 0.25. (We do not assess the significance of these skill metrics as this requires a formal estimate of independence in the observations. Our intent here is to use the skill to compare competing models.) If the dune height is omitted, the LRR skill drops to 0.5 while the CVI skill drops to 0.1. The value of the spatially varying uncertainty that accompanies each prediction is illustrated by comparing the weighted skill values (which use the confidence band to give more weight to more confident predictions). The unweighted skill values are always less than the weighted skill values. This indicates that the more confident predictions are actually more accurate. The LR score is positive for the LRR data set, explicitly indicating that the prediction is more accurate than using the prior probability of shoreline-change rate and the prediction is also more confident than the prior. The LR score is negative for the CVI data that are predicted with the BN trained on the LRR data, indicating poor accuracy, overconfidence, or both. The situation is similar if the BN is trained only on the CVI data and tested against the LRR data. To create a reliable model (which was used to generate the results shown in Figures 2, 5–7), the data sets are assimilated into one model. This reduces the skill (0.3 against both data sets) but the LR score is positive for both, indicating predictions that are accurate and confident. Using the model trained on both CVI and LRR data, the dune height predictions (Figure 7) were evaluated (Table 2). Predictions with either LRR or CVI shoreline-change rate as input were similar and dune height was predicted with a higher skill (about 0.6) compared with shoreline-change rates. Removing the shoreline-change rate reduced prediction skill only slightly (Table 2, "none" case).

The predictive skill for shoreline-change rate was low, but comparable to the skill obtained for the Gulf of Mexico region using a model that assimilated data from many coastlines, not just the Gulf of Mexico [*Gutierrez et al.*, 2014]. So far, we used a BN that was less complex than that used previously [*Gutierrez et al.*, 2011, 2014] because we chose to restrict the input to just two bins. We explored BN models with more bins per variable and this analysis showed that the hindcast skill increased until there are four to five bins per input. (More details of finding an optimal BN are presented in Section 4) The hindcast skill for the shoreline-change rates for the optimized BN (Figure 5c) increased to 0.6 (Table 1) and the skill was less sensitive to including or omitting the dune-height input. The corresponding dune-height prediction skill was nearly 0.8 (Table 2). The increased resolution of the input variables, particularly SLR, explained more variability of both data sets and was sufficient to provide improved prediction skill for shoreline change and dune height without

needing one to explicitly support the prediction of the other. Also, the LR increased, indicating improved confidence of the predictions even if the accuracy was not improved when one variable is used to predict the other.

3.3. Forecast Scenarios

The optimized model was used to predict shoreline-change rate, dune height, and corresponding shoreline-position changes in the future for two SLR scenarios. At this stage of the analysis we focus on a sub-region between Chandeleur Island, LA and Apalachicola, FL (Figure 1, main panel and inset 1), where the results of the present method have been used in two related studies [*Bilskie et al.*, 2016; *Passeri et al.*, 2016]. The first scenario replaces the observed relative SLR rate [i.e., the spatially varying rate, *Thieler and Hammar-Klose*, 1999] with a spatially uniform value of 1.8 mm/year, which is the approximate 20th century global average rate of SLR [*Church and White*, 2011] and is generally lower than the historical rate (3.9 mm/year, the average of values obtained from *Gutierrez et al.* [2014]) in the sub-region. The second scenario, corresponding to the average SLR for 2050 to 2100 "intermediate low" scenario of *Parris et al.* [2012], increased the SLR rate to 6.2 mm/year, which is generally higher than the observed rates. These scenarios can be applied to the entire domain, but we restrict our analysis to the sub-region to illustrate the impact of the different scenarios.

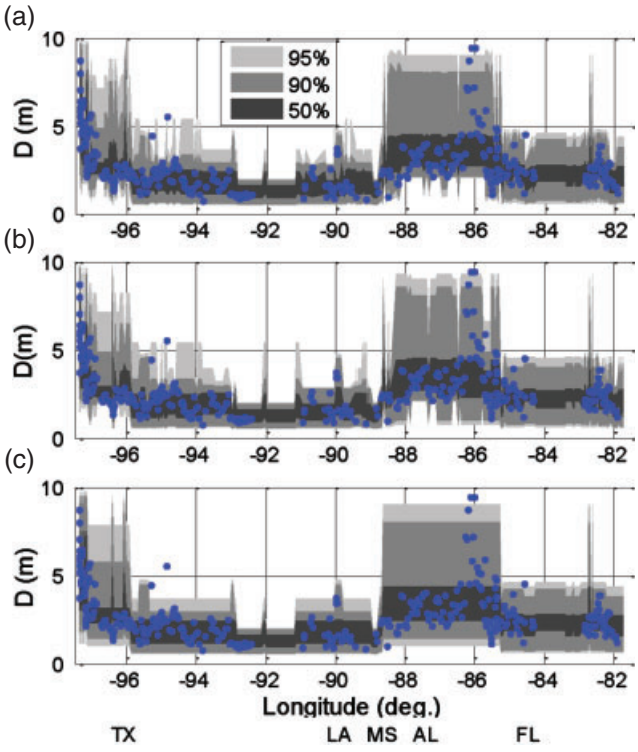

Figure 7. Dune-height prediction using Bayesian network trained with linear regression rate (LRR) and coastal vulnerability index (CVI) data and using (a) LRR data as input, (b) the CVI data as input, and (c) omitting any shoreline-change rate input. Blue dots represent the data. Abbreviations for each coastal state (TX, LA, MS, AL, and FL) are labeled for location reference (and see Figure 1).

Compared with the predictions and observations based on the historical SLR rate, the predicted shoreline-change rate becomes more negative (indicating increased erosion). The change is, on average, from −1.9 to −3.4 m/year (Table 3). In addition, the uncertainty of the prediction, measured as the average standard deviation of the prediction, increases from 4.4 to 6.5 m/year under the higher SLR scenario. The spatial variability of the forecast becomes generally more uniform as a result of the increased uncertainty (Figure 8). There is a region of the Florida coast (near 85° longitude) that is an exception to this generalization, where extremely confident predictions of no-change were made. By inspecting the data used to build the BN, we find that there are two actual locations that match the input SLR conditions corresponding to this scenario. The first is along the Texas coast near Matagorda (Figure 1, inset 2), where the shoreline change is between −1 and 0 m/year [*Miller et al.*, 2004]. The other location with relatively high SLR is the Chandeleur Islands (Figure 1) off the coast of Louisiana, which is eroding rapidly. In this prediction example, the dune-height prediction is confident that dunes will be about 2.5 m high (Figures 8e) and this interacts with the shoreline-change prediction to yield a scenario that is more similar to the Texas coast than the Chandeleur Islands as a whole.

The dune-height prediction at the location with the confident no-change prediction is accurate (Figure 8b), hence, we conclude that the scenario is a valid solution. Overall, the dune height is predicted to be reduced by about 1 m for the high SLR scenario, and dune height would increase, relative to current conditions, by about half a meter for the low SLR scenario (Table 3). The dune-height prediction is actually more confident

Table 1. Shoreline-Change Rate Prediction Statistics With (Without) Dune-Height Input

Hindcast Data	LR	Weighted Skill	Unweighted Skill
Model trained on LRR data			
LRR	55 (34)	0.64 (0.47)	0.30 (0.24)
CVI	−568 (−139)	0.25 (0.14)	0.07 (0.07)
Model trained on CVI data			
LRR	−184 (−9)	0.18 (0.15)	0.07 (0.06)
CVI	83 (58)	0.39 (0.16)	0.24 (0.17)
Model trained on LRR and CVI data			
LRR	33 (19)	0.33 (0.22)	0.20 (0.14)
CVI	65 (50)	0.32 (0.16)	0.19 (0.16)
Optimized model trained on LRR and CVI data			
LRR	45 (28)	0.65 (0.62)	0.44 (0.42)
CVI	78 (63)	0.56 (0.49)	0.26 (0.24)

CVI, coastal vulnerability index; LRR, linear regression rate.

Table 2. Dune-Height Prediction Statistics

Erosion Rate Input	LR	Weighted Skill	Unweighted Skill
Model trained on LRR and CVI data			
LRR	68	0.56	0.49
CVI	69	0.61	0.48
None	54	0.52	0.41
Optimized model trained on LRR and CVI data			
LRR	99	0.78	0.51
CVI	97	0.78	0.51
None	82	0.74	0.47

CVI, coastal vulnerability index; LRR, linear regression rate.

Table 3. Forecast Mean Shoreline-Change Rates and Dune-Crest Heights (Standard Deviation in Parentheses)

SLR Scenario	*E* (m/year)	*D* (m)	Δ2050 (m)
Optimized model trained on LRR and CVI data			
Observed (3.9 mm/year)	−1.1 (2.6)	3.2 (1.5)	—
Historical SLR	−1.9 (4.4)	3.5 (1.7)	−58 (234)
1.8 mm/year	−0.8 (2.7)	3.9 (2.0)	−32 (197)
6.2 mm/year	−3.4 (6.5)	2.4 (1.2)	−88 (281)

The mean and standard deviations of the data are listed for the observed scenario. The average of the prediction and the average of the prediction uncertainty are listed for the other scenarios.
CVI, coastal vulnerability index; LRR, linear regression rate; SLR, sea-level rise.

for the high SLR scenario (average standard deviation is 1.2 m) compared with either the hindcast or the low SLR scenario. Note that dune-height predictions depend on shoreline change, sea-level, storms, and other factors, but do not have an explicit time component because we do not estimate rates of dune-height change. This exposes an implied assumption that dunes will respond rapidly and be in equilibrium with the SLR and shoreline-change rates. See Section 4 for further elaboration of this point.

The prediction of the change in shoreline position (employing equation (1a)), evaluated in the year 2050 shows that the mean prediction is about 90 m of erosion (Table 3) under the high SLR rate and just 30 m of erosion under the low SLR rate. Any other year could be selected, and we included 2100 as a target when

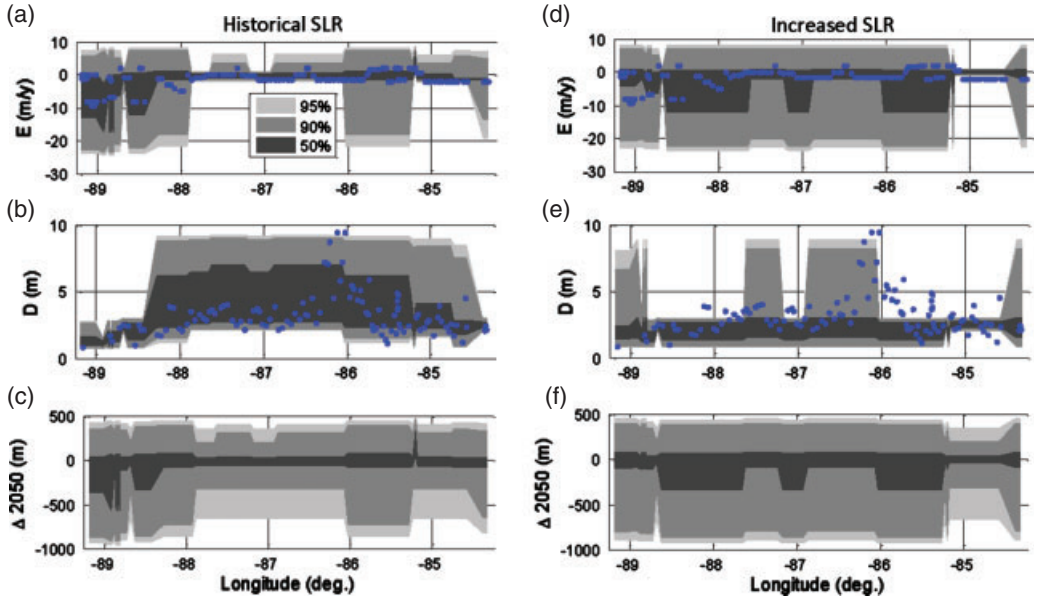

Figure 8. Forecast scenarios for the historical sea-level rise (SLR) rate (a–c) and future scenario with 6.2 mm/year SLR rate (d–f). Predictions are of the shoreline-change rate, *E*, dune-crest height, *D*, and change in shoreline position, Δ. The data (blue dots) are shown as a reference to historical conditions. Shading is same scale as shown in Figures 6 and 7.

we applied this method in related studies [*Bilskie et al.*, 2016; *Passeri et al.*, 2016]. The uncertainty in the shoreline-change rate prediction is propagated to the shoreline change and we see that there is higher uncertainty with the high SLR rate (Table 3, Figure 8). In fact, the uncertainty is so high in most locations that there is more than a 10% chance that the shoreline could recede by over 500 m (Figure 8f), which may exceed the actual barrier width. This implies either that there could be significant barrier island migration, barrier island loss (e.g., similar to that projected by *Gutierrez et al.* [2009] for the U.S. Mid-Atlantic barrier islands), or, particularly where there is infrastructure or important ecosystems, that humans may engineer the coast at these locations should a high SLR rate affect this region [*Reed and Wilson*, 2004].

4. Discussion

We have developed an enhanced, statistical prediction of shoreline-change rates that can utilize dune height as input, predict the dune height using shoreline change (and other variables) as input, or predict shoreline change and dune height simultaneously and consistently. Using a BN approach to develop statistical predictions allows assimilation of data from a wide area (much of the U.S. Gulf of Mexico coastline) that spans diversity in shoreline-change rates (including multiple data sets), geomorphology, dune height, tidal and wave conditions, and relative SLR. We show that prediction skill can be improved most by optimizing the BN model to improve the resolution of the input variables. With the optimized model, the primary value of including dune height to predict shoreline-change rates (and vice versa) was to improve the prediction confidence. Prediction confidence is important to understand for future scenarios where we use the model to predict response to higher SLR rates. Here, we discuss in detail the optimized model, the role, and origin of dune-height and shoreline-change rate correlations, and the implications of the results with respect to understanding uncertainty for decision making and understanding the outcome of complicated geomorphological processes.

The optimized model had increased resolution of most inputs variables and was capable of making the most skillful predictions of both shoreline change and dune heights. One explanation for the improved skill of the optimized model is that it simply over-fit the data and was not robust. This is almost always true to some extent. We evaluated the degree of overfitting using a calibration/validation approach [*Fienen and Plant*, 2015] that trained the model on a portion of the shoreline-change data and tested it on a withheld portion (Figure 9). The validation was performed by training on two-thirds of the data, and testing on the remaining, withheld third of the data set, and doing this for all three permutations of training and testing

data. The skill statistic was then averaged across all three permutations. The calibration skill improved as the number of bins increased until about five bins. The bin boundaries were automatically assigned to give equal prior probability to each bin. The validation skill improved most when four bins were used, and then degraded as the number of bins increased. Hence, the optimal model has four input bins (Figure 5c), except for the geomorphology and slope variables, which, as already mentioned, had very little variability and were well resolved with just two bins.

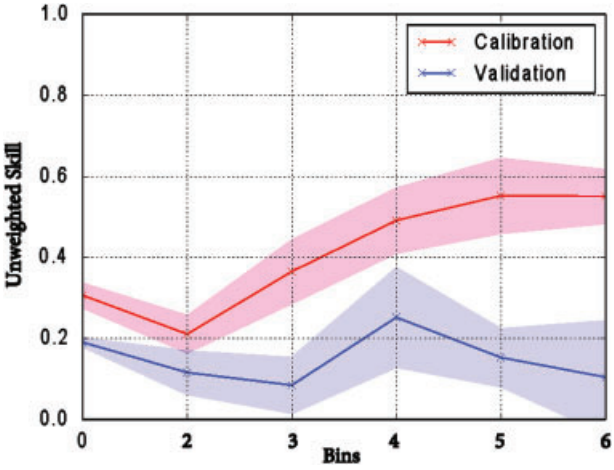

Figure 9. Shoreline-change rate calibration and validation test showing the change in skill with increase in the resolution of the Bayesian network (BN)'s input variables. The first test, indicated by "0" bins, is the baseline two-bin BN. The shaded areas indicate the minimum and maximum from all three calibration/validation permutations.

The baseline BN (plotted at "0" bins coordinate for comparison in Figure 9) included two bins for all input variables and actually had a validation skill that was twice as good as the skill estimated using the automatically generated, two-bin and three-bin BNs. This suggests that there are important thresholds in the input variables that were resolved in the baseline net, but not in the automatically generated two-bin and three-bin nets. Adding more bins ensures that these thresholds are resolved. For example, the baseline net split SLR bins at 6 mm/year while the automatically generated net split SLR bins at 4 mm/year (giving an equal number of data points above and below this threshold). Because there is a large amount of scatter in the relationship between shoreline change and SLR (Figure 3), the higher threshold used in the baseline net gave a stronger shoreline-change rate response. Similarly, joint correlations between SLR, shoreline-change rate, and dune height point to generally lower dunes if SLR > 5 mm/year — resolving this threshold behavior is important for improving the prediction skill.

By testing how much all variables contributed to uncertainty reduction in both the baseline and optimized BNs [*Marcot et al.*, 2006; *Norsys Software Corp*, 2012], we found that SLR was the most important input for shoreline-change rate and dune-height predictions. The next most important variables were dune height to predict shoreline-change rate and vice versa. We showed in the hindcast tests that, for the optimized model, the addition of one variable (dune height or shoreline-change rate) as input to predicting the other did not substantially improve the predictive skill. This reflects the joint correlation between all three variables (*E*, *D*, and SLR), suggesting that when any two are known, the third is redundant. While dune height does not contribute much to prediction skill, the prediction confidence was improved, as indicated by increases in the LR (by 30% for shoreline change and by 20% for dune-height). This result makes sense because the uncertainty can be reduced by adding redundant information with independent errors. For example, dune heights greater than 4–5 m are strongly correlated with lower shoreline-change rates and lower SLR rates (Figure 4). On the other hand, lower dune heights are associated with rapidly eroding shorelines (and higher SLR rates) but there is also higher uncertainty in these relationships. The conditional probabilities of these two cases results in variable uncertainty estimates and the LR metric measures how well these variations are predicted.

Understanding prediction uncertainty is important for the forecasting applications (e.g., coastal resource management decisions) because there will be (1) uncertainty in the future conditions (such as SLR) and (2) uncertainty in the coastline response even if the future conditions are known. Some components of spatial and temporal variability in dune heights are an intrinsic and likely unpredictable feature of barrier islands, as demonstrated by analysis of historical observations [*Gutierrez et al.*, 2015] and recent experiments [*Lazarus and Armstrong*, 2015]. The BN approach is capable of propagating the first type of uncertainty to describe its impact on the second type. Uncertainty in shoreline-change rate and, therefore, shoreline positions tended to increase under the higher SLR scenario (Figures 8d and 8f). However, high SLR was likely to lead to a

confident prediction of low dune heights (Figure 8e). Thus, the BN approach can be used to determine the likelihood of negative outcomes. A high likelihood of extreme outcomes (e.g., shoreline erosion and low dunes) can result from high uncertainty (the outcome cannot be ruled out) and high confidence (e.g., low dunes). Another application of probabilistic predictions that account for joint correlation is to provide specific shoreline change and dune-height scenarios [e.g., to support more detailed modeling investigations, *Passeri et al.*, 2016] that are mutually consistent and consistent with future SLR. Hence, this model approach has broad value in characterizing future modification of the coast given a wide range of possible SLR rates that are represented in many SLR projections [e.g., *Parris et al.*, 2012].

The joint correlation between dune height, SLR, and shoreline-change rate can be interpreted as the statistical representation of morphologic feedbacks. Capturing these relationships can support both statistical models, as used here, and idealized dynamical models [e.g., *Lorenzo-Trueba and Ashton*, 2014]. For statistical models, correlations can be related to causation (i.e., physical processes), such as major storms, that drive shoreline and dune-height changes. For much of the northern Gulf of Mexico, a typical hurricane is expected to yield combined extreme water levels, including storm surge and wave runup, that reach about 4 m in elevation [*Stockdon et al.*, 2012]. For coastlines with dunes that are lower than this level, each hurricane can be expected to cause dune overwash barrier-island rollover, and shoreline retreat. The combination of storms and SLR will drive future changes [*Wahl and Plant*, 2015]. This may explain why dune height did not contribute much to shoreline-change predictions skill (and vice versa). If the dunes respond rapidly to the combined impacts of SLR and storms, then they will be in statistical equilibrium with the longer-term processes. This may also be true for accreting and eroding shorelines. Our predictions of shoreline change under high SLR resulted in an increased probability of shoreline accretion as well as erosion, even if erosion is more likely (Figure 5a). Under high SLR, regardless of whether the shoreline is accreting or eroding, the dune heights were most likely to be low. A physical explanation is that accreting coastlines allow foredune growth, which depends on positive sand supply and a wide beach, among other factors [*Durán and Moore*, 2013; *Zarnetske et al.*, 2015]. The dune-crest height data that we used always corresponded to the seaward most dune [*Stockdon et al.*, 2009], which may be newly formed and relatively low on accreting coasts. Thus, under high SLR, dunes are either overwashed often and this reduces their height or the coast is evolving rapidly and this also maintains a low elevation. This is a possible explanation for the high confidence in low dune heights under the future SLR scenario.

We acknowledge that we do not explicitly incorporate physical processes, which typically requires a model that conserves fluxes of fluid momentum and sediment. But this is not our intent. Instead, we use observations of the real coastal system to identify multivariate states that emerge from natural (or even combined natural and anthropogenic) processes. Our modeling approach resolved 900 different possible states, which is the number of possible combinations of input and output bins for which conditional probabilities are computed in the baseline BN—there are 3256 possible states in the optimized BN. There were 565 data locations and seven variables, yielding approximately 3900 data values used to calibrate the BNs. Many of the conditional probabilities were nearly zero and it is possible to train a model with more states than data points if the true correlations are localized in the BN parameter space. Where the correlations are not localized, our approach identifies results for which we may want to develop a better process-based understanding that demonstrates improved predictive skill and reduced uncertainty.

5. Conclusions

Previous work has demonstrated that spatial variability of long-term shoreline change can be predicted using observed SLR rates, average tide range, wave height, coastal slope, and a characterization of the geomorphic setting. We compared two different data sets describing centennial-scale shoreline change in the Gulf of Mexico and showed that about 40% of the data variance was correlated to each other and both data sets were assimilated into a predictive model because it was not clear that one data set was more accurate than the other. The correlations of each data set to other variables (SLR and dune height) were similar (e.g., Figures 3 and 4). We developed an enhanced BN model that includes coastal dune height as a way to add additional information to improve shoreline-change predictions. Dune height is also intrinsically important for predicting changes in storm vulnerability as sea level rises. We showed that adding dune-height information improves the prediction skill of shoreline-change rates only if the BN under-resolves the input variables. The under-resolved model illustrated broad trends in the joint correlation between the primary variables

of interest (SLR, shoreline change, and dune height, Figure 5), but predictions explained only 30% and 50% of shoreline-change rate and dune-height variability, respectively. An optimized model was developed for application to forecasting scenarios and it predicted dune height with better skill (0.8) compared with shoreline change (0.6). In the optimized model, the value of using dune height to predict shoreline-change rates (and vice versa) was to reduce prediction uncertainty while having little impact on prediction skill (Tables 1 and 2). The predictive model can be implemented with a range of forecast scenarios, and we illustrate this by imposing two SLR rates, one that was low and one that was high. Predicted shoreline-change rates were extrapolated to predict future shoreline positions. Future conditions may lead to more uncertainty in some predictions (e.g., shoreline change under high SLR) and reduced uncertainty in other predictions (dune heights under high SLR). Thus, forecast predictions can be used to evaluate the probability of adverse impacts of future SLR and to select mutually consistent shoreline-change and dune-height scenarios under future SLR.

Acknowledgments

We are indebted to our colleagues Ben Gutierrez and Erika Lentz for their roles in guiding our BN model developments. Specifically, Ben has demonstrated to us the value of using storm-related metrics (e.g., dune height) along with long-term change metrics that have been part of our earlier collaboration. Erika exposed the fact that the BN approach included several types of mathematical operations, and that not all of them actually rely on Bayes rule. We are also grateful for the efforts of Elizabeth Pendleton, who assembled much of the data that we relied on and Peter Howd who assembled the data for the first incarnation of the BN model that we utilized here. Thomas Wahl reviewed an early draft of the manuscript and we thank him and two anonymous reviewers for their careful reading and constructive comments that improved the clarity and accuracy of this paper. This work was supported by the USGS Coastal and Marine Geology Program and the USGS Southeast Regional Assessment Project. All data for this paper are properly cited and referred to in the reference list. The use of trade, firm, or product names is for descriptive purposes only and does not imply endorsement by the U.S. Government.

References

Apotsos, A., B. Raubenheimer, S. Elgar, and R. T. Guza (2008), Testing and calibrating parametric wave transformation models on natural beaches, *Coastal Eng.*, *55*, 224–235, doi:10.1016/j.coastaleng.2007.10.002.

Atkinson, J. H., J. M. Smith, and C. Bender (2013), Sea-level rise effects on storm surge and nearshore waves on the Texas coast: influence of landscape and storm characteristics, *J. Waterw. Port Coastal Eng.*, *139*(2), 98–117, doi:10.1061/(asce)ww.1943-5460.0000187.

Bilskie, M. V., S. C. Hagen, S. C. Medeiros, and D. L. Passeri (2014), Dynamics of sea level rise and coastal flooding on a changing landscape, *Geophys. Res. Lett.*, *41*(3), 927–934, doi:10.1002/2013GL058759.

Bilskie, M. V., S. C. Hagen, K. Alizad, S. C. Medeiros, D. L. Passeri, H. F. Needham, and A. Cox (2016), Dynamic simulation and numerical analysis of hurricane storm surge under sea level rise with geomorphologic changes along the northern Gulf of Mexico, *Earth's Future*, *4*, doi:10.1002/2015EF000347.

Church, J. A., and N. J. White (2011), Sea-level rise from the late 19th to the early 21st century, *Surv. Geophys.*, *32*, 585–602, doi:10.1007/s10712-10011-19119-10711.

Church, J. A., et al. (2013), Sea level change. *Climate Change 2013: The Physical Science Basis, Contribution of Working Group I to the Fifth Assessment Report of the Intergovernmental Panel on Climate Change*, Stocker, T.F., D. Qin, G.-K. Plattner, M. Tignor, S.K. Allen, J. Boschung, A. Nauels, Y. Xia, V. Bex *and* P.M. Midgley Cambridge Univ. Press, Cambridge, UK and New York.

Dempster, A. P., N. M. Laird, and D. B. Rubin (1977), Maximum likelihood from incomplete data via the EM algorithm, *J. R. Stat. Soc. Ser. B*, *39*(1), 1–38.

Donnelly, C., N. Kraus, and M. Larson (2006), State of knowledge on measurement and modeling of coastal overwash, *J. Coastal Res.*, *22*(4), 965–991, doi:10.2112/04-0431.1.

Doran, K. S., H. F. Stockdon, N. G. Plant, A. H. Sallenger, K. K. Guy, and K. A. Serafin (2009), Hurricane Gustav: observations and analysis of coastal change, *U.S. Geol. Surv. Open-File Rep. OFR-2009-1279*, 28 p., U.S. Geological Survey, Reston, Va.

Durán, O., and L. J. Moore (2013), Vegetation controls on the maximum size of coastal dunes, *Proc. Natl. Acad. Sci. U. S. A.*, *110*(43), 17217–17222, doi:10.1073/pnas.1307580110.

Fearnley, S. M., M. D. Miner, M. Kulp, C. Bohling, and S. Penland (2009), Hurricane impact and recovery shoreline change analysis of the Chandeleur Islands, Louisiana, USA: 1855 to 2005, *Geo-Mar. Lett.*, *29*, 455–466, doi:10.1007/s00367-009-0155-5.

Fienen, M. N., and N. G. Plant (2015), A cross-validation package driving Netica with python, *Environ. Modell. Software*, *63*, 14–23, doi:10.1016/j.envsoft.2014.1009.1007.

Gulf Coast Ecosystem Restoration Council (2014), FY2014 annual report to Congress, https://www.restorethegulf.gov/sites/default/files/FY2014AnnualReportToCongress.pdf, 20 pp.

Gutierrez, B. T., S. J. Williams, and E. R. Thieler (2009), *Ocean Coasts, in Coastal Sensitivity to Sea-Level Rise: A Focus on the Mid-Atlantic Region* , pp. 43–56, U.S. Clim. Change Sci. Program, Washington, D.C.

Gutierrez, B. T., N. G. Plant, and E. R. Thieler (2011), A Bayesian network to predict the coastal vulnerability to sea-level rise, *J. Geophys. Res.: Earth Surf.*, *116*(F02009), 1–15, doi:10.1029/2010JF001891.

Gutierrez, B. T., N. G. Plant, E. A. Pendleton, and E. R. Thieler (2014), Using a Bayesian network to predict shore-line change vulnerability to sea-level rise for the coasts of the United States, *U.S. Geol. Surv. Open File Rep. 2014–1083*, 26 pp., U.S. Geological Survey, Reston, Va.

Gutierrez, B. T., N. G. Plant, E. R. Thieler, and A. Turecek (2015), Using a Bayesian network to predict barrier island geomorphologic characteristics, *J. Geophys. Res.: Earth Surf.*, *120*, 1–24, doi:10.1002/2015JF003671.

Guy, K. K., H. F. Stockdon, N. G. Plant, K. S. Doran, and K. L. M. Morgan (2013), Hurricane Isaac—observations and analysis of coastal change, *U.S. Geol. Surv. Open File Rep. 2013–1270*, 21 p., U.S. Geological Survey, Reston, Va.

Hagen, S. C., and P. Bacopoulos (2012), Coastal flooding in Florida's Big Bend region with application to sea level rise based on synthetic storms analysis, *Terr. Atmos. Ocean Sci.*, *23*, 481–500, doi:10.3319/tao.2012.04.17.01(wmh).

Lauritzen, S. L. (1995), The EM algorithm for graphical association models with missing data, *Comput. Stat. Data Anal.*, *19*, 191–201, doi:10.1016/0167-9473(93)e0056-a.

Lazarus, E. D., and S. Armstrong (2015), Self-organized pattern formation in coastal barrier washover deposits, *Geology*, *43*(4), 363–366, doi:10.1130/g36329.1.

Lindemer, C. A., N. G. Plant, J. A. Puleo, D. M. Thompson, and T. V. Wamsley (2010), Numerical simulation of a low-lying barrier island's morphological response to Hurricane Katrina, *Coastal Eng.*, *57*(11–12), 985–995, doi:10.1016/j.coastaleng.2010.06.004.

Long, J. W., A. T. M. d. Bakker, and N. G. Plant (2014), Scaling coastal dune elevation changes across storm-impact regimes, *Geophys. Res. Lett.*, *41*, doi:10.1002/2014GL059616, 1–8 pp.

Lorenzo-Trueba, J., and A. D. Ashton (2014), Rollover, drowning, and discontinuous retreat: distinct modes of barrier response to sea-level rise arising from a simple morphodynamic model, *J. Geophys. Res.: Earth Surf.*, *119*, 779–801, doi:10.1002/2013JF002941.

Marcot, B. G., J. D. Steventon, G. D. Sutherland, and R. K. McCann (2006), Guidelines for developing and updating Bayesian belief networks applied to ecological modeling and conservation, *Can. J. For. Res.*, *36*, 3063–3074, doi:10.1139/x06-135.

McCall, R. T., J. S. M. Van Thiel de Vries, N. G. Plant, A. R. Van Dongeren, J. A. Roelvink, D. M. Thompson, and A. J. H. M. Reniers (2010), Two-dimensional time dependent hurricane overwash and erosion modeling at Santa Rosa Island, *Coastal Eng.*, *57*(7), 668–683, doi:10.1016/j.coastaleng.2010.02.006.

Miller, T. L., R. A. Morton, A. H. Sallenger, and L. J. Moore (2004), The National Assessment of Shoreline Change: a GIS compilation of vector shorelines and associated shoreline change data for the U.S. Gulf of Mexico, *USGS Open File Rep. 2004–1089*, 45 p., U.S. Geological Survey, Reston Va.

Moore, L. J., P. Ruggiero, and J. H. List (2006), Comparing mean high water and high water line shorelines: should proxy-datum offsets be incorporated into shoreline change analysis? *J. Coastal Res.*, *22*(4), 894–905, doi:10.2112/04-0401.1.

Morton, R., T. Miller, and L. Moore (2004), National assessment of shoreline change: part 1: historical shoreline changes and associated coastal land loss along the U.S. Gulf of Mexico, *U.S. Geol. Surv., Open-File Rep. 2004-1043*, 43 p., U.S. Geological Survey, Reston, Va.

Mousavi, M. E., J. L. Irish, A. E. Frey, F. Olivera, and B. L. Edge (2011), Global warming and hurricanes: the potential impact of hurricane intensification and sea level rise on coastal flooding, *Clim. Change*, *104*(3–4), 575–597, doi:10.1007/s10584-009-9790-0.

Norsys Software Corp (2012), Netica 5.05, Norsys Software Corp, Vancouver, Canada.

Parris, A.P., et al. (2012), Global sea level rise scenarios for the US National Climate Assessment, *NOAA Tech Memo OAR CPO-1*, 37 p., National Oceanic and Atmospheric Administration, Silver Springs, Md.

Passeri, D. L., S. C. Hagen, and J. L. Irish (2014), Comparison of shoreline change rates along the South Atlantic Bight and Northern Gulf of Mexcico coasts for better evaluation of future shoreline positions under sea-level rise, *J. Coastal Res.*, *SI-68*, 20–26, doi:10.2112/sI68-003.1.

Passeri, D. L., S. C. Hagen, S. C. Medeiros, and M. V. Bilskie (2015a), Impacts of historic morphological changes and sea level rise on tidal hydrodynamics in the Grand Bay, Mississippi estuary, *Cont. Shelf Sci.*, *111*(Part B), 150–158, doi:10.1016/j.csr.2015.08.001.

Passeri, D. L., S. C. Hagen, M. V. Bilskie, and S. C. Medeiros (2015b), On the significance of incorporating shoreline changes for evaluating coastal hydrodynamics under sea level rise scenarios, *Nat. Hazards*, *75*(2), 1599–1617, doi:10.1007/s11069-014-1386-y.

Passeri, D. L., S. C. Hagen, N. G. Plant, M. V. Bilskie, S. C. Medeiros, and K. Alizad (2016), Tidal hydrodynamics under future sea level rise and coastal morphology in the Northern Gulf of Mexico, *Earth's Future*, *4*, doi:10.1002/2015EF000332.

Penland, S., R. Boyd, and J. Suter (1988), Transgressive depositional systems of the Mississippi delta plain: model for barrier shoreline and shelf sand development, *J. Sediment. Petrol.*, *58*, 932–949.

Plant, N. G., and H. F. Stockdon (2012), Probabilistic prediction of barrier-island response to hurricanes, *J. Geophys. Res.: Earth Surf.*, *117*(F03015), 1–17, doi:10.1029/2011JF002326.

Plant, N. G., H. F. Stockdon, A. H. Sallenger, M. J. Turco, J. W. East, A. A. Taylor, and W. A. Shaffer (2010), Forecasting hurricane impact on coastal topography, *Eos Trans. AGU*, *91*(7), 65–66, doi:10.1029/2010EO070001.

Plant, N. G., J. Flocks, H. F. Stockdon, J. W. Long, K. Guy, D. M. Thompson, J. M. Cormier, C. G. Smith, J. L. Miselis, and P. S. Dalyander (2014), Predictions of barrier island berm evolution in a time-varying storm climatology, *J. Geophys. Res.: Earth Surf.*, *119*, 300–316, doi:10.1002/2013JF002871.

Priestly, M. B. (1981), *Spectral Analysis and Time Series*, 890 pp., Academic Press, London.

Reed, D. J., and L. Wilson (2004), Coast 2050: a new approach to restoration of Louisiana coastal wetlands, *Phys. Geogr.*, *25*(1), 4–21, doi:10.2747/0272-3646.25.1.4.

Roelvink, J. A., A. Reniers, A. V. Dogeren, J. V. T. d. Vries, R. McCall, and J. Lescinski (2009), Modeling storm impacts on beaches, dunes and barrier islands, *Coastal Eng.*, *56*, 1133–1152, doi:10.1016/j.coastaleng.2009.08.006.

Sallenger, A. H., Jr. (2000), Storm impact scale for barrier islands, *J. Coastal Res.*, *16*(3), 890–895.

Sallenger, A. H., Jr., C. W. Wright, P. Howd, K. Doran, and K. Guy (2009), Extreme coastal changes on the Chandeleur Islands, Louisiana, during and after Hurricane Katrina, in *Sand Resources, Regional Geology, and Coastal Processes of the Chandeleur Islands Coastal System—An Evaluation of the Breton National Wildlife Refuge: U.S. Geol. Surv. Sci. Invest. Rep. 2009–5252*, edited by D. Lavoie, U.S. Geological Survey, Reston VA, pp. 27–36.

Sherwood, C. R., J. W. Long, P. J. Dickhudt, P. S. Dalyander, D. M. Thompson, and N. G. Plant (2014), Inundation of a barrier island (Chandeleur Islands, Louisiana, USA) during a hurricane: observed water-level gradients and modeled seaward sand transport, *J. Geophys. Res.: Earth Surf.*, *119*, 1–18, doi:10.1002/2013JF003069.

Smith, J. M., M. A. Cialone, T. V. Wamsley, and T. O. McAlpin (2010), Potential impact of sea level rise on coastal surges in southeast Louisiana, *Ocean Eng.*, *37*, 37–47.

Stockdon, H. F., A. H. Sallenger Jr., R. Holman, and P. Howd (2007), A simple model for the spatially-variable coastal response to hurricanes, *Mar. Geol.*, *238*, 1–20, doi:10.1016/j.margeo.2006.11.004.

Stockdon, H. F., K. S. Doran, and A. H. Sallenger Jr. (2009), Extraction of lidar-based dune-crest elevations for use in examining the vulnerability of beaches to inundation during hurricanes, *J. Coastal Res.*, *53*, 59–65, doi:10.2112/sI53-007.1.

Stockdon, H. F., K. J. Doran, D. M. Thompson, Sopkin K.L., N. G. Plant, and A. H. Sallenger (2012), National assessment of hurricane-induced coastal erosion hazards: Gulf of Mexico, *U.S. Geol. Surv. Open File Rep. 2012–1084*, 51 pp.

Stolper, D., J. H. List, and E. R. Thieler (2005), Simulating the evolution of coastal morphology and stratigraphy with a new morphological-behaviour model (GEOMBEST), *Mar. Geol.*, *218*(1–4), 17–36, doi:10.1016/j.margeo.2005.02.019.

Thieler, E. R., and E. S. Hammar-Klose (1999), National assessment of coastal vulnerability to sea-level rise: preliminary results for the U.S. Atlantic Coast, *U.S. Geol. Surv. Open File Rep. 99-593*, http://pubs.usgs.gov/of/1999/of99-593/.

Twichell, D. C., E. Pendleton, W. Baldwin, and J. Flocks (2009), Subsurface control on seafloor erosional processes offshore of the Chandeleur Islands, Louisiana, *Geo Mar. Lett.*, *29*(6), 349–358, doi:10.1007/s00367-009-0150-x.

Twichell, D. C., J. G. Flocks, E. A. Pendleton, and W. E. Baldwin (2013), Geologic controls on regional and local erosion rates of three Northern Gulf of Mexico barrier-island systems, *J. Coastal Res.*, *SI-63*, 32–45, doi:10.2112/si63-004.1.

Wahl, T., and N. G. Plant (2015), Changes in erosion and flooding risk due to long-term and cyclic oceanographic trends, *Geophys. Res. Lett.*, 2943–2950, doi:10.1002/2015gl063876.

Weigend, A. S., and R. J. Bhansali (1994), Paradigm change in prediction, *Philos. Trans. R. Soc. Lond. Ser. A-Math. Phys. Eng. Sci.*, *348*(1688), 405–420, doi:10.1098/rsta.1994.0100.

Zarnetske, P. L., P. Ruggiero, E. W. Seabloom, and S. D. Hacker (2015), Coastal foredune evolution: the relative influence of vegetation and sand supply in the US Pacific Northwest, *J. R. Soc. Interface*, *12*(106), doi:10.1098/rsif.2015.0017.